Available online at www.sciencedirect.com
ScienceDirect
Journal of Environmental Sciences 2011, 23(5) 798–807
JOURNAL OF ENVIRONMENTAL SCIENCES
ISSN 1001-0742
CN 11-2629/X
www.jesc.ac.cn

Effects of continuously regenerating diesel particulate filters on regulated emissions and number-size distribution of particles emitted from a diesel engine

Zhihua Liu[1,2], Asad Naeem Shah[1,3], Yunshan Ge[1,*], Yan Ding[4], Jianwei Tan[1], Lei Jiang[1], Linxiao Yu[1], Wei Zhao[1], Chu Wang[1], Tao Zeng[1]

1. School of Mechanical Engineering, Beijing Institute of Technology, Beijing 100081, China. E-mail: liuzhihua161@163.com
2. Bourns College of Engineering, Center for Environmental Research and Technology, and Department of Chemical and Environmental Engineering, University of California, Riverside, CA 92507, USA
3. Department of Mechanical Engineering, University of Engineering and Technology, Lahore 54000, Pakistan
4. Chinese Research Academy of Environmental Sciences, Beijing 100012, China

Received 19 May 2010; revised 14 June 2010; accepted 23 June 2010

Abstract

The effects of continuously regenerating diesel particulate filter (CRDPF) systems on regulated gaseous emissions, and number-size distribution and mass of particles emanated from a diesel engine have been investigated in this study. Two CRDPF units (CRDPF-1 and CRDPF-2) with different specifications were separately retrofitted to the engine running with European steady-state cycle (ESC). An electrical low pressure impactor (ELPI) was used for particle number-size distribution measurement and mass estimation. The conversion/reduction rate (R_{CR}) of hydrocarbons (HC) and carbon monoxide (CO) across CRDPF-1 was 83% and 96.3%, respectively. Similarly, the R_{CR} of HC and CO and across CRDPF-2 was 91.8% and 99.1%, respectively. The number concentration of particles and their concentration peaks; nuclei mode, accumulation mode and total particles; and particle mass were highly reduced with the CRDPF units. The nuclei mode particles at downstream of CRDPF-1 and CRDPF-2 decreased by 99.9% to 100% and 97.8% to 99.8% respectively; and the particle mass reduced by 73% to 92.2% and 35.3% to 72.4%, respectively, depending on the engine conditions. In addition, nuclei mode particles increased with the increasing of engine speed due to the heterogeneous nucleation initiated by the higher exhaust temperature, while accumulation mode particles were higher at higher loads due to the decrease in the air-to-fuel ratio (A/F) at higher loads.

Key words: diesel engine; regulated emissions; particulate matter; number-size distribution; continuously regenerating diesel particulate filter

DOI: 10.1016/S1001-0742(10)60452-4

Citation: Liu Z H, Naeem Shah A, Ge Y S, Ding Y, Tan J W, Jiang L et al., 2011. Effects of continuously regenerating diesel particulate filters on regulated emissions and number-size distribution of particles emitted from a diesel engine. Journal of Environmental Sciences, 23(5): 798–807

Introduction

The forthcoming tighter emission standards for diesel engines are a challenge for researchers working with diesel exhaust emissions, and demand for developing high-efficient after-treatment devices and retrofitting to diesel engines is increasing. Among these after-treatment units, continuously regenerating diesel particulate filter (CRDPF) has proved to be a very effective and promising technology for the abatement of particulate matter (PM) emissions from diesel engines. This technique not only reduces PM mass, but also provides good control over the number of ultrafine particles (Lanni et al., 2001).

PM emissions from diesel engines consist mainly of carbon soot, volatile organic fraction (VOF), and small amount of sulfate, and nitrate species (Kittelson et al., 2006), which have adverse effects on the environment as well as human health. Soot is black carbon consisting of a large number of ultra-fine particles less than 100 nm in size which are dominant in diesel exhaust, can absorb sunlight and thus contribute to global warming (Kittelson et al., 2006).

Wong et al. (2003) reported that diesel exhaust particles consist of nuclei, accumulation, and coarse modes with diametric ranges of 5–50 nm, 50–1000 nm, and more than 2.5 μm, respectively. The nuclei mode particles contribute only 1%–20% of total particle mass, but are responsible for nearly 90% of total particle number. The ultra-fine particles, especially nuclei mode particles, are detrimental to human health as they have a high probability of inhalation,

* Corresponding author. E-mail: geyunshan@bit.edu.cn

and hence most likely cause inflammation, respiratory diseases, and lung cancer (Donaldson et al., 1998). It is critical to measure particle number instead of their mass for future emission legislation since toxicity increases as the size distribution of particles decreases (Tsolakis, 2006).

The CRDPF system uses nitrogen dioxide (NO_2) to combust the soot collected in a particulate filter (Cooper and Thoss, 1989). This oxidation of carbon by NO_2 occurs at about 250°C, which is achievable under normal driving conditions, particularly in heavy duty engine applications (Walker et al., 2003). This NO_2-based combustion at such low temperature leads to the development of a diesel particulate filter (DPF) technology that will continue to burn the PM trapped during normal working conditions. As a result, the DPF will continuously regenerate and maintain an acceptable low back pressure. The regeneration of a CRDPF unit is sensitive to sulfur content, and is adversely affected by the increased amount of sulfur in the fuel (Walker et al., 2002).

A continuously regenerating trap (CRT) or CRDPF unit has a diesel oxidation catalyst (DOC) which converts not only nitric oxide (NO) to NO_2, but also oxidizes HC and CO ideally to carbon dioxide (CO_2) and water (H_2O). Therefore, this system has the advantage of controlling PM, CO, and HC emissions simultaneously.

The current work focuses on the impact of CRDPF units on the control of regulated gaseous emissions and PM mass. The role of CRDPF technology in the abatement of nuclei and accumulation mode particles were also addressed. Furthermore, we attempted to examine the brake specific fuel consumption (BSFC) with and without the CRDPF systems to investigate engine fuel economy.

1 Materials and methods

1.1 Test bench, engine type, fuel and operating cycle

Figure 1 presents the experimental bench, consisting of an engine coupled with CRDPF after-treatment technology and dynamometer (Schenck HT 350, Germany). It also shows the sampling scheme for measuring regulated gaseous emissions, and analysis of number-size distribution of the particles before and after the CRDPF system.

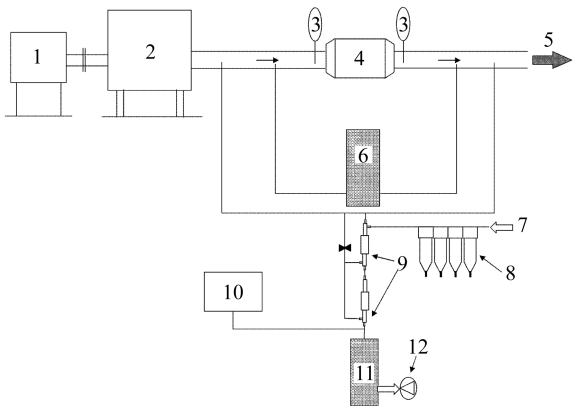

Fig. 1 Experimental setup. (1) dynamometer; (2) diesel engine; (3) temperature and pressure sensors; (4) DPF system, (5) exhaust out; (6) AMA4000; (7) compressed air in; (8) air filters; (9) diluter; (10) CO_2 analyzer (SEMTECH-DS); (11) ELPI; (12) vacuum pump.

The engine used in this study was a 4-stroke 4-cylinder turbocharged inter-cooled diesel engine (specifications in Table 1). The engine was fueled with locally available commercial diesel with properties and standards listed in Table 2. The air flow rate, fuel flow rate, engine oil and coolant temperatures, and exhaust temperature were measured using Sensyflow P (ABB Inc., Switzerland), PLU4000 (PierBerg, Austria), and thermocouple, respectively.

The experiments were performed in accordance with 13-mode European steady state cycle (ESC) (Table 3). According to the test cycle, the engine was run at a speed N_A = 2125 r/min at 100%, 75%, 50%, and 25% of full load for mode 2, 6, 5 and 7, respectively. It was then operated at N_B = 2660 r/min at 100%, 75%, 50%, and 25% of full load during the modes 8, 4, 3, and 9, respectively. Finally, it was run at N_C = 3200 r/min at 100%, 75%, 50%, and 25% of full load for mode 10, 12, 13, and 11, respectively.

1.2 DPF systems and their specifications

We used two commercial traps, the CRDPF-1 from China and CRDPF-2 from South Korea, in this study. The

Table 1 Engine specifications

Parameter	Feature/Value
Engine type	Diesel, 4-stroke, 4-cylinders in-line
Air intake system	Inter-cooled, turbocharged
Fuel metering system	High pressure common rail
Valves	Two valves per cylinder
Capacity	2.771 L
Bore	93 mm
Stroke	102 mm
Compression ratio	18.2:1
Rated power	(75 kW)/(3600 r/min)
Maximum torque	(250 N·m)/(1900 r/min)

Table 2 Properties of fuels

Properties	Diesel	Test method
Lower heating value	42.8 MJ/kg	GB/T 384
Density	841 kg/m^3	SH/T 0604
Viscosity at 20°C	4 mm^2/sec	GB/T 265
Cetane number	52	GB/T 386-91
Sulfur content	350 ppm	SH/T 0253-92
Hydrogen content	13%	SH/T 0656-98
Carbon content	87%	SH/T 0656-98
Oxygen content	0%	Elemental analysis

Table 3 European steady-state cycle (ESC) test parameters

Parameter	Speed (r/min)	Torque (N·m)	Power (kW)
P_{max}	3600	200	75
50% P_{max}	1540	232.5	37.5
70% P_{max}	3880	129.2	52.5
A*	2125	230	51.2
B	2660	220	61.3
C	3200	210	70.4
Idle	800	0	0

*A is the point between 50% P_{max} and point B, where B is the point between 50% P_{max} and 70% P_{max}, and C is the point between B and 70% P_{max}.

Table 4 Specifications of the CRDPF systems

Parameter	CRDPF-1	CRDPF-2
DOC substrate	Metal	Cordierite
DOC cell density (cells/inch^2)	600	400
DOC Pt. content (g/ft^3)	50	50
Diameter × Length (inch × inch)	8.5 × 3.5	8.5 × 3.5
DPF substrate	Cordierite	Cordierite
DPF cell density (cells/inch^2)	100	200
DPF Pt. content (g/ft^3)	35	35
Diameter × Length (inch × inch)	8.5 × 14	8.5 × 14

1 inch = 2.54 cm.

specifications of both after treatment units are in Table 4. These units were made up of two chambers where the soot trapping/combustion step was proceeded by the oxidation process in the inlet. The first DOC chamber serves the purpose of NO oxidation to NO_2 for the burning/combustion of soot. It also oxidizes HC, CO, and a portion of the PM known as solid (SOL). The second chamber was comprised of a ceramic wall-flow filter that permits exhaust to flow through it. The filter was also of honeycomb design, wherein alternate channels were blocked at one end, and thus the exhaust was forced to flow through the walls of the filter. In this way, gaseous components of the exhaust passed through the walls, while soot was trapped. The soot was then burned or combusted continuously by NO_2 generated by the DOC. This generated NO_2 was capable of combusting soot at a lower temperature, compared with oxygen (O_2). In a CRDPF unit, inlet head, outlet head, catalyst and filter sections were built with stainless steel. The V-clamps were used to connect all above modules of the unit.

1.3 Sampling and measuring of pollutants

The engine exhaust was sampled both upstream and downstream of the CRDPF (Fig. 1). Regulated gaseous emissions such as HC, CO, and oxides of nitrogen (NO*x*) were measured using an exhaust analyzer AVL AMA4000 (AVL, Austria). An ELPI (Dekati Ltd., Finland) was used to investigate particle number-size distributions, and hence mass estimation by inserting a J-shaped stainless steel sampler probe into the exhaust pipe (Jiang et al., 2010). Before starting the experimentation, the dilutor was calibrated using two concentrations of CO_2 measured before and after the dilutor. The overall dilution ratio was about 56. The analytical package AMA4000 (the error of all analyzer ≤ 0.5% of the measure value add 2 times detect limits) and SEMTECH-DS were used for this purpose.

2 Results and discussions

2.1 Regulated gaseous pollutants

2.1.1 HC emissions

Figure 2 shows the upstream and downstream HC emissions with CRDPF-1 and CRDPF-2 separately, together with their corresponding conversion/reduction rate (R_{CR}) defined as Eq. (1):

$$R_{CR} = \frac{(U_s - D_s)}{U_s} \times 100\% \quad (1)$$

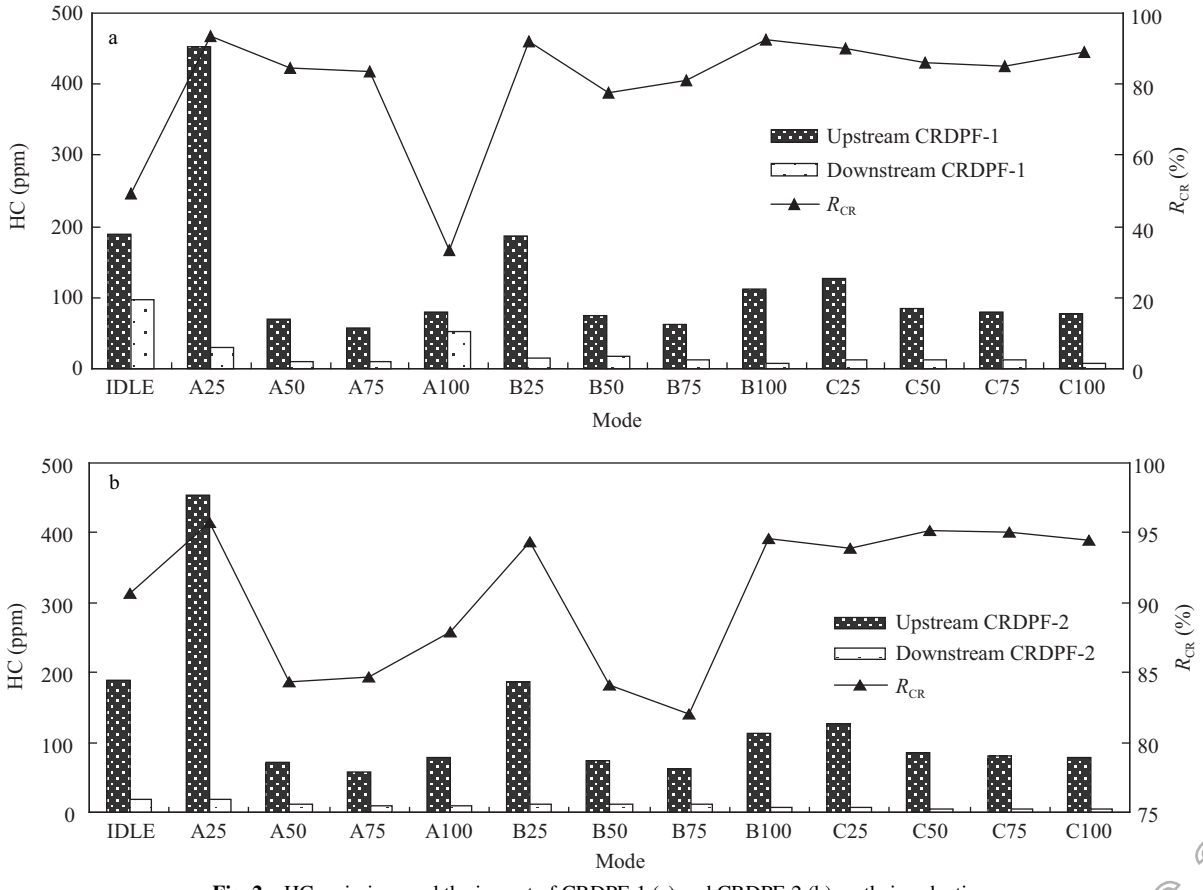

Fig. 2 HC emissions and the impact of CRDPF-1 (a) and CRDPF-2 (b) on their reduction.

where, U_s and D_s are the pollutants measured upstream and downstream of the CRDPF systems, respectively. The pollutant conversion or controlling rate across CRDPF-1 and CRDPF-2 varied from 33.2% (at mode A100) to 93.4% (at mode A25) and from 82% (at mode B75) to 95.8% (at mode A25) during the ESC cycle. This reduction was attributed to the oxidation of HC pollutants ideally to H_2O and CO_2 in the presence of DOC. The increase in downstream CO_2 of the CRDPF units relative to their corresponding upstream CO_2 (Table 5) indicated the conversion of HC emissions into CO_2 across the CRDPF traps.

It is obvious from Fig. 2 that HC emissions were higher at lower load than higher load. The higher HC emissions at lower loads were attributed to incomplete combustion caused by the over-lean mixture area or the larger air-to-fuel (A/F) ratio developed in the combustion chamber of the engine, as shown in Table 5. The presence of over-lean mixture in the combustion chamber slows down the flame propagation and reaction, resulting in the formation of incomplete combustion products (Heywood, 1988).

It is worth noting that CR of HC pollutants across the CRDPF-1 was higher compared to CRDFF-2. This may be due to the different specifications of the two traps. The DOC cell density of CRDPF-1 was also higher than CRDPF-2 (Table 4).

2.1.2 CO emissions

As presented in Fig. 3, the CO emissions greatly reduced downstream of the CRDPFs, and hence R_{CR} was remarkably high. R_{CR} value varied from 31.7% (at mode A100) to 99.7% (at mode A25) and from 97.6% (at mode A100)

Table 5 Air/fuel (A/F) ratio and CO_2 concentration (%, Vol) at various modes of European steady-state cycle test

	U_s	D_{s1}	D_{s2}	U_s	D_{s1}	D_{s2}	U_s	D_{s1}	D_{s2}	U_s	D_{s1}	D_{s2}
	Mode A25			Mode A50			Mode A75			Mode A100		
A/F	48.2	47.6	49.6	36.4	37.6	37.1	30.8	32.3	32.0	24.9	28.6	25.7
CO_2	3.53	4	3.82	5.09	5.19	5.16	6.01	6.10	6.04	7.58	7.59	7.60
	Mode B25			Mode B50			Mode B75			Mode B100		
A/F	54.2	55.4	55.5	37.9	40.1	39.4	31.2	32.9	32.3	25.4	27.3	26.4
CO_2	3.33	3.51	3.43	4.83	4.86	4.87	5.95	6.00	5.99	7.41	7.39	7.46
	Mode C25			Mode C50			Mode C75			Mode C100		
A/F	52.9	54.1	53.4	36.2	37.4	37.6	28.5	29.7	29.7	23.4	24.8	24.4
CO_2	3.42	3.58	3.52	5.05	5.18	5.10	6.53	6.62	6.54	8.06	7.98	8.07

U_s: pollutants measured upstream; D_s: pollutants measured downstream.

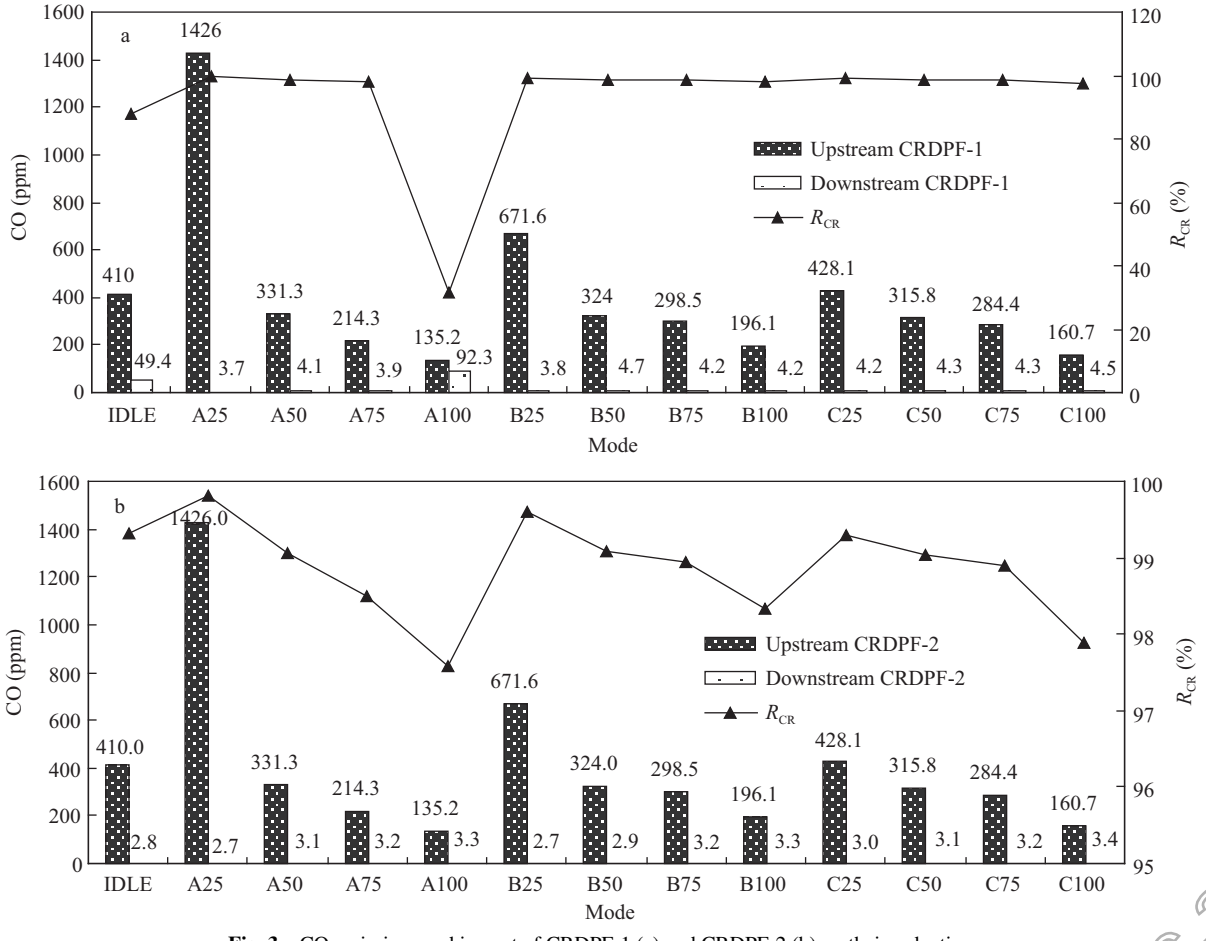

Fig. 3 CO emissions and impact of CRDPF-1 (a) and CRDPF-2 (b) on their reduction.

to 99.8% (at mode A25) with CRDPF-1 and CRDPF-2, respectively. The reductions in CO emissions were due to the oxidation of CO into CO_2 across the CRDPFs. The increase in downstream CO_2 (Table 5) was most likely due to the oxidation of CO and HC emissions not the oxidation of PM, since PM contribution to the formation of CO_2 is insignificant (Thalagavara et al., 2005).

It is obvious from Fig. 3 that CO emissions tended to decrease with the increase in load for N_A, N_B and N_C of the ESC test. The higher CO emissions at lower loads were ascribed to the development of a lean mixture area in the cylinder at lower loads because the rate of fuel oxidation and decomposition depends on unburned gaseous fuel and mixture temperature formed in the cylinder (Kouremenos et al., 1999). Both of these parameters contributed to the formation CO pollutants. However, the better oxidation caused by the increase in load, thereby decrease in A/F ratio, results in the decrease of CO emissions. This decrease in CO results in the increase of CO_2.

2.1.3 NO*x* emissions

Figure 4 reflects the emissions of NO*x* pollutants before and after the CRDPF systems, and the R_{CR} value of these pollutants at various modes of the ESC test. At some modes, NO*x* conversion was positive, while at others their CR was negative with both of the CRDPF systems. This leads to reluctance for conversion of NO*x* at some modes of the test cycle. As far as the positive conversion or simply conversion is concerned, R_{CR} fluctuated from 1.7% to 34.2% and 0.4% to 20% with CRDPF-1 and CRDPF-2, respectively. On the other hand, the negative conversion or simply reluctance varied from 0.9% to 45.2% and 0.5% to 6% across the CRDPF-1 and CRDPF-2, respectively.

The NO*x* emissions showed haphazard trends for their CR across the CRDPFs. Although they revealed significant reduction at some modes, their overall R_{CR} was very low. However, CRDPF-2 exhibited comparatively better control on NO*x* emissions. The difference in the CR trends with the two CRDPFs was attributed to their different specifications.

It is worth noting that NO*x* pollutants were lower at lower load modes. They tended to increase with the increase in load level and, thus reached maximum at full load modes for N_A, N_B and N_C of the ESC test. The maximum NO*x* pollutants at full load were probably due to the higher combustion temperature at full loads compared lower loads.

According to the ESC test results in Table 6, the R_{CR} of HC and CO pollutants across the CRDPF-1 was 83% and 96.3%, respectively, while the R_{CR} across the CRDPF-2 were 91.8% and 99.1%, respectively. However, the CRDPF systems did not show any significant impact on NO*x* emissions. Therefore, a reluctance or negative conversion of 0.1% and a R_{CR} of only 3.5% was obtained with CRDPF-1 and CRDPF-2, respectively. These findings are in good agreement with previous studies (Walker et al., 2002; LeTavec et al., 2000), in which the CRDPF systems gave more than 90% reductions in PM, HC and CO emissions

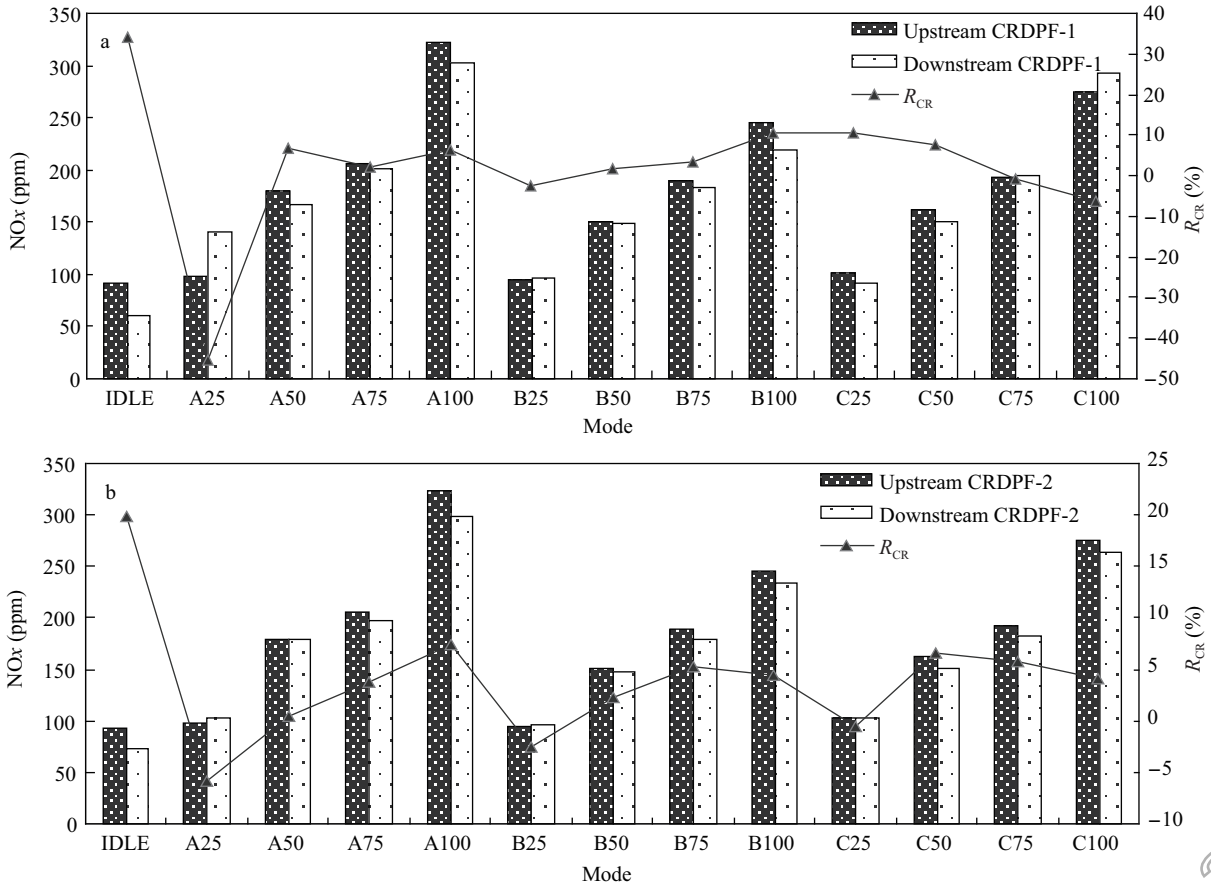

Fig. 4 NO*x* emissions and the impact of CRDPF-1 (a) and CRDPF-2 (b) on their reduction.

Table 6 European steady-state cycle test results

Pollutant	BSE (g/(kW·hr))			Conversion rate (%)	
	U_s in CRDPF	D_s in CRDPF-1	D_s in CRDPF-2	CRDPF-1	CRDPF-2
HC	0.52	0.09	0.04	83.0	91.8
CO	3.34	0.12	0.03	96.3	99.1
NO*x*	2.99	300	2.89	–0.1	3.5

BSE: brake specific emissions.

without any significant abatement in NO*x* pollutants. The possible reason for a nominal or even negative conversion of NO*x* might be the conversion of other nitrogen oxides (such as N_2O) to NO or NO_2 after CRDPF units, which cannot be measured by AMA4000.

2.2 Number concentration and size distribution of the particles

Figure 5 presents the comparison of number-size distribution of particles before and after the CRDPF systems for various modes of the cycle. The particle diameters range from 7 nm to 10 μm. Number-concentration of nuclei mode particles was obviously higher both upstream and downstream of the CRDPF traps, while the downstream number-concentration of particles decreased significantly over the entire range of diameters. In addition, the downstream number concentration peaks were lower with both CRDPF units at all modes of the three cyclic speeds. Furthermore, upstream number distributions were unimodal, while downstream distributions were bimodal and unimodal for CRDPF-1 and CRDPF-2, respectively.

As presented in Table 7, the upstream nuclei mode particles were major contributors to the total number of particles at most cyclic modes. This may be due to the soluble organic fraction (SOF) and rapid nucleation of particles, which nucleate during the dilution process as the diesel exhaust comes out the tail pipe (Kati et al., 2004). Further, the downstream nuclei mode particles were generally higher compared to the corresponding accumulation mode particles for both CRDPF systems. We attributed this to the removal of carbonaceous particles across the CRDPF traps. In the absence of carbonaceous particles, both the sulfates and HC form nuclei mode particles (Thalagavara et al., 2005). Furthermore, homogenous nucleation caused plays an important role in increasing nuclei mode particles because if volatile material does not find soot surface for adsorption, the HC condensation possibility increases (Armas et al., 2008).

It is important to note that both nuclei and accumulation mode particles decreased across the CRDPF units. These reductions were highly profound for CRDPF-1 compared to CRDPF-2. The reduction in number concentration of nuclei mode particles varied from 99.9% to 100% and 98.4% to 99.8% across the CRDPF-1 and CRDPF-2,

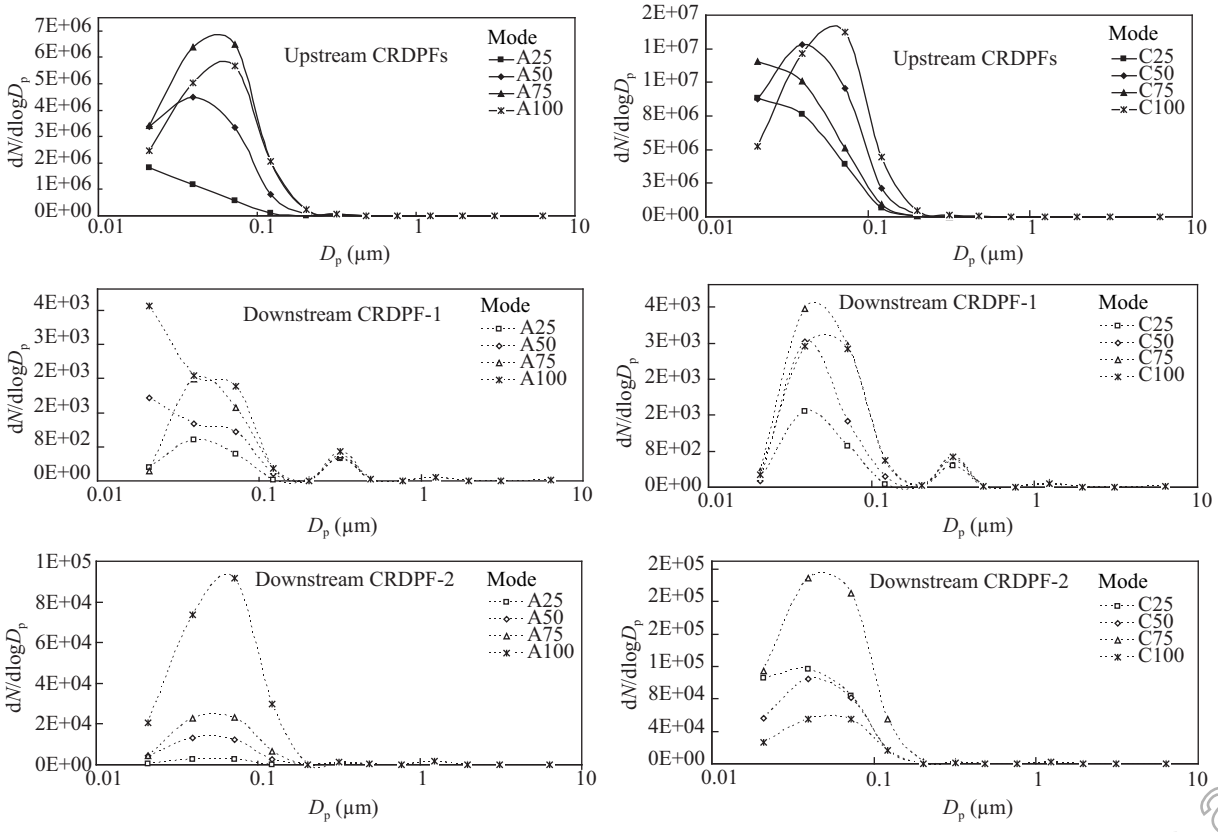

Fig. 5 Number-size distribution of the particles upstream and downstream of the CRDPFs.

Table 7 Number of particles in nuclei and accumulation modes

	U_s	D_{s1}	D_{s2}	U_s	D_{s1}	D_{s2}
	Mode A25			Mode A50		
Nuclei mode	2.98E+06	1.28E+03	3.01E+03	7.86E+06	3.28E+03	1.73E+04
Accumulation mode	7.10E+05	1.19E+03	3.67E+03	4.25E+06	1.88E+03	1.54E+04
Total	3.69E+06	2.55E+03	8.08E+03	1.21E+07	5.27E+03	3.42E+04
	Mode A75			Mode A100		
Nuclei mode	9.79E+06	2.60E+03	2.70E+04	7.49E+06	6.56E+03	9.43E+04
Accumulation mode	8.85E+06	2.64E+03	3.07E+04	8.05E+06	3.25E+03	1.23E+05
Total	1.86E+07	5.35E+03	5.94E+04	1.55E+07	9.93E+03	2.19E+05
	Mode B25			Mode B50		
Nuclei mode	9.90E+06	1.79E+03	1.73E+04	1.93E+07	3.57E+03	9.03E+04
Accumulation mode	2.81E+06	1.38E+03	9.01E+03	1.34E+07	2.72E+03	5.51E+04
Total	1.27E+07	3.25E+03	2.76E+04	3.27E+07	6.39E+03	1.47E+05
	Mode B75			Mode B100		
Nuclei mode	1.87E+07	5.29E+03	7.18E+04	1.48E+07	3.84E+03	5.72E+04
Accumulation mode	1.75E+07	3.64E+03	5.18E+04	1.64E+07	4.14E+03	5.21E+04
Total	3.63E+07	9.05E+03	1.25E+05	3.11E+07	8.08E+03	1.11E+05
	Mode C25			Mode C50		
Nuclei mode	1.64E+07	1.87E+03	2.23E+05	2.15E+07	3.38E+03	1.62E+05
Accumulation mode	4.69E+06	1.46E+03	1.02E+05	1.20E+07	2.33E+03	1.01E+05
Total	2.11E+07	3.41E+03	3.26E+05	3.35E+07	5.79E+03	2.64E+05
	Mode C75			Mode C100		
Nuclei mode	2.16E+07	4.31E+03	3.44E+05	1.74E+07	3.40E+03	8.21E+04
Accumulation mode	6.17E+06	4.41E+03	2.70E+05	1.88E+07	4.41E+03	7.26E+04
Total	2.78E+07	8.83E+03	6.16E+05	3.62E+07	7.91E+03	1.56E+05

respectively. The decrease in number concentration of accumulation mode particles ranged from 99.8% to 100% and from 95.6% to 99.7% with CRDPF-1 and CRDPF-2, respectively. Consequently, total number of particles decreased by 99.9% to 100% and 97.8% to 99.8% across CRDPF-1 and CRDPF-2, respectively. These findings are in good agreement with previous research (Lanni et al., 2001) demonstrating that particle trapping efficiency of CRDPF was at least 99%. The decrease in nuclei mode particles was likely due to the decrease in SOF with the CRDPF traps. On the other hand, the decrease in accumulation mode particle may be attributed to SOL of PM, and it is probable that SOL also decreased with the CRDPF units.

In general, upstream accumulation mode particles and total number of particles were higher at higher load modes compared to lower ones (Table 7). This was attributed to higher fuel injection or decrease in A/F ratio causing incomplete or partial combustion of carbonaceous PM, as carbonaceous particulate results from diffusion combustion, which is enhanced when more fuel is injected into the cylinder after ignition (Warner et al., 2003; Heywood, 1988).

It is concerning to note that the upstream nuclei particles, in particular, and the downstream particles, in general, increased with engine speed for all four load levels of the cycle (Table 7). This was most likely due to the heterogeneous nucleation initiated by higher exhaust temperature developed at increased speeds. This higher temperature leads to the conversion of SO_2 to SO_3 on the catalyst. The generated SO_3 is then converted to sulfuric acid nuclei during the cooling process accomplished by the dilution air. The sulfuric acid nuclei act as condensation nuclei of the volatile organic material available in the sample (Armas et al., 2008). This adsorption phenomenon produced on the nuclei of inorganic compounds (such as sulfuric acid or water) is responsible for higher nuclei mode particles at higher speeds, relative to lower ones. According to Giechaskiel et al. (2005), the combination of oxidation catalyst and fuel having a certain content of sulfur can promote the formation of nuclei mode particles.

It is worth mentioning that in spite of the use of conventional low sulfur fuel (350 ppm) in this research, particle trapping efficiency of the CRDPF systems was remarkably high, which means that CRDPF retrofits can also provide very good capturing efficiency even with conventional low sulfur diesel fuel. Although the two CRDPFs showed a small difference in their trapping efficiencies, they played a significant role in the reduction of both nuclei and accumulation mode particles. This reduction was attributed to the higher reduction rates of HC emissions (Fig. 2). Further, it is probable that the volatile fraction of PM decreases in the presence of CRDPF technology, thereby diesel exhaust particles decreases.

2.3 Particle mass estimation

An ELPI was used to estimate particle mass of the exhaust by assuming particle density as the function of their size. This assumption plays a critical role in the particle mass estimation and may cause the overestimation of their mass (Tsukamato et al., 2000; Abdul-Khaliq, 2000). However, this method can provides an opportunity to make

the comparison between upstream and downstream mass concentrations of the particles. In this study, the effective density of diesel particles was assumed as 1 g/cm^3 and only stage 1–7 of EPLI were taken into account while the particles were considered spherical in shape. The use of unit density was in agreement with other studies (Tsolakis et al., 2006). The assumption that particles were of spherical shape was also consistent with other studies. Lanni et al. (2001) reported that there are almost no carbon particles in the gas-phase and liquid material to adsorb onto or coalesce around in case of CRDPF system. So, the average particle diameter does not grow and remains small, resulting in the formation of only spherical collector particles.

Figure 6 shows that particle mass was highly reduced across the CRDPF systems. The R_{CR} varied from 73% (mode A25) to 92.2% (mode C100) and 35.3% (mode A25) to 72.4% (C100) across the CRDPF-1 and CRDPF-2, respectively. The R_{CR} was minimal at lower load modes, while it was maximal at higher load modes of the cyclic speeds. This was probably due to the decrease in the oxidation rate of NO to NO_2 at lower loads compared to higher ones. The higher loads generated higher temperature in the combustion chamber, which increased oxidation of NO to NO_2. This then helped in the oxidation of carbonaceous PM across the diesel particulate traps (Thalagavara et al., 2005), and thereby may have decreased the particle mass.

It can be seen from Fig. 6 that upstream particle mass increased with the increase in engine load for all three variably-loaded speeds of the cycle, with the exception of mode C75. This may be due to the increase in fuel flow rate in the cylinder or decrease in A/F ratio, which may result in higher soot emissions and, thus higher particle mass at higher loads compared to lower ones. Dec et al. (1997) reported that the products of fuel-rich mixture contain an abundance of unburned fuel, and their flames are hot enough to accomplish fuel pyrolysis and soot formation.

2.4 Brake specific fuel consumption (BSFC)

Trapped soot has the tendency to block filters and affect the engine performance. Therefore, it is necessary for the captured soot to be combusted in time to avoid choking the filter. Filter blockage increases the exhaust back pressure on the engine, and hence may adversely affect the economy of the engine. As such, we calculated the BSFC of the engine, as shown in Fig. 7. The BSFC was almost the same with and without CRDPF-1, and the difference remained within ±1.5% at all cyclic modes with the exception of mode A25 (4.3%). In the case of CRDPF-2, there was a marginal change in the BSFC and the difference remained within ±1% throughout the test cycle. From the above discussion, it can be deduced that CRDPF retrofitting does not cause any serious harm to the fuel economy of the engine.

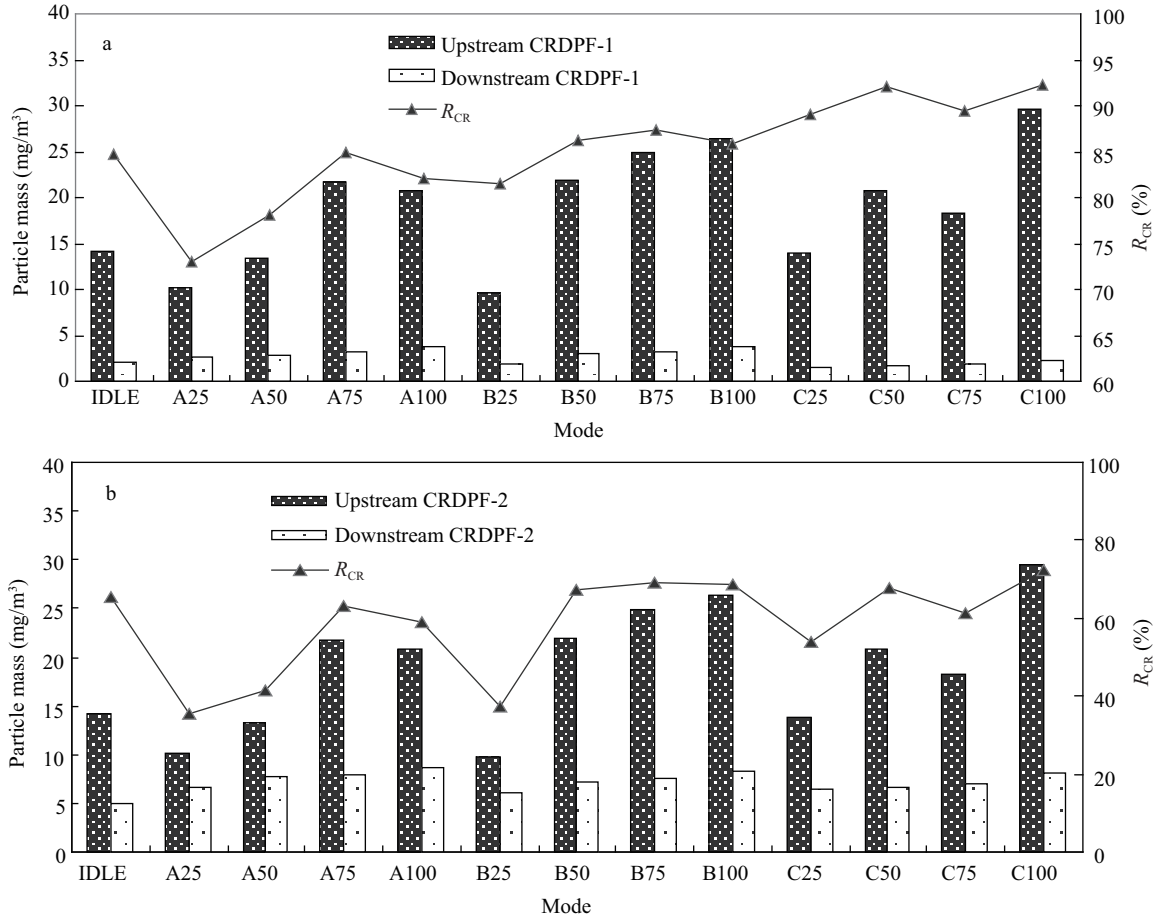

Fig. 6 Particle mass and the impact of CRDPF-1 (a) and CRDPF-2 (b) on their reduction.

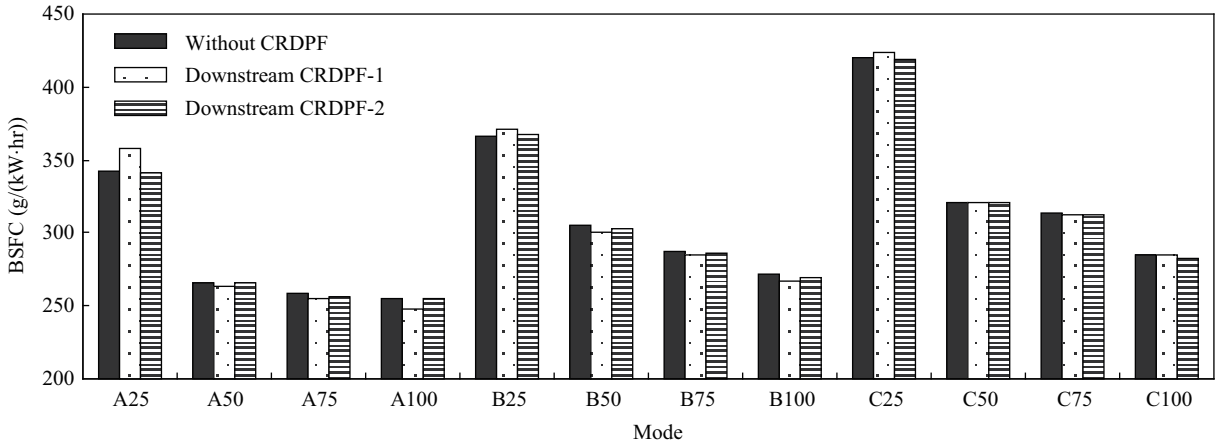

Fig. 7 Brake specific fuel consumption (BSFC) of the engine with and without CRDPF-1 and CRDPF-2.

3 Conclusions

Two CRDPF systems were investigated to examine their impact on controlling regulated gaseous emissions, and the number-size distribution and mass of particles from diesel engine exhaust. The CRDPF exhibited strong impact on the conversion of HC and CO emissions, but no significant impact on the conversion of NOx pollutants. According to the ESC test results, the conversion of HC, CO, and NOx across the CRDPF-1 was 83%, 96.3% and –0.1% respectively, while CR across the CRDPF-2 was 91.8%, 99.1% and 3.5% respectively.

Furthermore, the nuclei and accumulation mode particles significantly decreased and, thus total number of particles decreased by 99.9% to 100% and 97.8% to 99.8% across the CRDPF-1 and CRDPF-2, respectively. In addition, the maximum CR of particle mass was above 92% and 72% across the CRDPF-1 and CRDPF-2, respectively. A positive correlation was found between load level and the R_{CR} of particle mass and, thus R_{CR} increased with load level increase. Generally, the upstream accumulation mode particles were higher at higher load modes compared to lower ones, while nuclei mode particles increased with the increase in cyclic speed. Although conventional low sulfur (350 ppm) fuel was used in the study, both CRDPF units exhibited remarkable particle trapping performance. The CRDPF retrofits did not reveal any significant increase in BSFC and fuel economy of the engine was very good.

Acknowledgments

This work was supported by the National Natural Science Foundation of China (No. 40805053). The authors gratefully acknowledge the technical support and guidelines of the Lab staff during the experiments.

References

Abdul-Khaliq I S, 2000. Characterization of particle size distribution of a heavy duty diesel engine during FTP transient cycle using ELPI. SAE Technical Paper Series No. 2000-01-2001.

Armas O, Ballesteros R, Gomez A, 2008. The effect of diesel engine operating conditions on exhaust particle size distributions. *Proceeding of the Institute of Mechanical Engineers, Part D: Journal Automobile Engineering*, 222: 1513–1525.

Cooper B J, Thoss J E, 1989. Role of NO in diesel particulate emission control. SAE Technical Paper Series No. 890404.

Dec J E, 1997. A conceptual model of DI diesel combustion based on laser sheet imagining. SAE Technical Paper Series No. 970873.

Donaldson K, Li X Y, MacNee W, 1998. Ultrafined (manometer) particle mediated lung injury. *Journal of Aerosol Science*, 29: 553–560.

Giechaskiel B, Ntziachristos L, Samaras Z, Scheer V, Casati R, Vogt R, 2005. Formation potential of vehicle exhaust nucleation mode particles on-road and in the laboratory. *Atmospheric Environment*, 39: 3191–3198.

Heywood J B, 1988. Internal Combustion Engine Fundamentals. McGraw-Hill, London.

Jiang L, Ge Y S, Shah A N, He C, Liu Z, 2010. Unregulated and unregulated emissions from a diesel engine equipped with vanadium-based urea-SCR catalyst. *Journal of Environmental Sciences*, 22(4): 575–581.

Kati V, Annele V, Jyrki R Jorma K, 2004. Effect of after-treatment system on size distribution of heavy duty diesel exhaust aerosol. SAE Technical Paper Series No. 2004-01-01980.

Kittelson D B, Watts W F, Johnson J P, Rowntree C J, Goodier S P, Payne M J et al., 2006. Driving down on-highway particulate emissions. SAE Paper No. 2006-01-0916

Kouremenos D A, Hountalas D T, Kouremenos A D, 1999. Experimental investigation of the effect of fuel composition in the formation of pollutants in direct injection diesel engines. SAE Technical Paper Series No. 1999-01-0527.

Lanni T, Chatterjee S, Conway R, Windawi H, Rosenblatt D, Bush C et al., 2001. Performance and durability evaluation of continuously regenerating particulate filters on diesel powered urban bused at NY City transit. SAE Technical Paper Series No. 2001-01-0511.

LeTavec C, Uihlein J, Segal J, Vertin K, 2000. EC-diesel technology validation program interim report. SAE Technical Paper Series No. 2000-01-1854.

Thalagavara A M, Johnson J H, Bagley S T, Shende A S, 2005. The effects of a catalyzed particulate filter and ultra low sulfur fuel on heavy duty diesel engine emissions. SAE Technical Paper Series No. 2005-01-0473.

Tsolakis A, 2006. Effects on particle size distribution from the diesel engine operating on RME-biodiesel with EGR. *Energy and Fuels*, 20: 1418–1424.

Tsukamato Y, Goto Y, Odaka M, 2000. Continuous measurement of diesel particulate emissions by an electrical low pressure impactor. SAE Technical Paper Series No. 2000-01-1138.

Walker A P, Allansson R, Blakeman P G, Lavenius M, Erkfeldt S, Landalv H et al., 2003. The development and performance of the compact SCR-trap system: A 4-way diesel emission control system. SAE Technical Paper Series No. 2003-01-0778.

Walker A P, Allansson R, Blakeman P G, Cooper B J, Hess H, Silcock P H, 2002. Optimizing the low temperature performance and regeneration efficiency of the continuously regenerating diesel particulate filter (Cr-Dpf) system. SAE Technical Paper Series No. 2002-01-0428.

Warner J R, Johnson J H, Bagley S T, Huynh C T, 2003. Effects of a catalyzed particulate filter on emissions from a diesel engine: Chemical characterization data and particulate emissions measured with thermal optical and gravimetric methods. SAE Technical Paper Series No. 2003-01-0049.

Wong C P, Chan T L, Leung C W, 2003. Characterization of diesel exhaust particle number and size distributions using mini-dilution tunnel and ejector-diluter measurement techniques. *Atmospheric Environment*, 37: 4435–4446.